

Searching for statistical equilibrium in a dynamical multifragmentation path

A. H. Raduta^{a,c}, M. Colonna^{a,b}, M. Di Toro^{a,b}

^a*LNS-INFN, via S.Sofia 62, I-95123, Catania, Italy*

^b*Physics and Astronomy Dept. University of Catania, Italy*

^c*NIPNE, RO-76900 Bucharest, Romania*

A method for identifying statistical equilibrium stages in dynamical multifragmentation paths as provided by transport models, already successfully tested for the reaction $^{129}\text{Xe} + ^{119}\text{Sn}$ at 32 MeV/u is applied here to a higher energy reaction, $^{129}\text{Xe} + ^{119}\text{Sn}$ at 50 MeV/u. The method evaluates equilibrium from the point of view of the microcanonical multifragmentation model (MMM) and reactions are simulated by means of the stochastic mean field model (SMF). A unique solution, corresponding to the maximum population of the system phase space, was identified suggesting that a huge part of the available phase space is occupied even in the case of the 50 MeV/u reaction, in presence of a considerable amount of radial collective flow. The specific equilibration time and volume are identified and differences between the two systems are discussed.

PACS numbers: 24.10.Pa; 25.70.Pq

I. INTRODUCTION

From more than 20 years, *statistical equilibrium* was a basic ingredient in many theoretical [1, 2, 3, 4, 5] and experimental nuclear multifragmentation studies. This was motivated by the good agreements obtained over the time between various observables related to the asymptotically resulted fragments and various statistical multifragmentation models.

However, the agreement in the asymptotic stage between experiments and statistical models predictions is only a *necessary* condition for equilibrium. For fully “proving” equilibrium one has to have direct access to the *primary decay* stage of the reaction. In fact, different primary configurations could lead to the same final results, because of compensative effects between primary and secondary emission mechanisms. Experimentally it is difficult to “measure” the primary decay stage: this signal is distorted by the secondary particle emission. An elegant solution is to perform a statistical analysis on the primary decay stage as predicted by a dynamical model yielding results in good agreement with experimental data. One of such models is the Stochastic Mean Field (SMF)[6, 7, 8].

In Ref. [9] a statistical analysis was performed on the dynamical path provided by SMF with the microcanonical multifragmentation model (MMM) [5]. There, an effective method for identifying the *equilibrated stage* in the dynamical path was proposed and successfully tested for the $^{129}\text{Xe} + ^{119}\text{Sn}$ at 32 MeV/u reaction. A fully equilibrated source was identified at 140 fm/c, with a corresponding volume of $3.4 V_0$ (where V_0 is the volume of the source at normal nuclear density). Herein we apply the same analysis to the higher energy reaction $^{129}\text{Xe} + ^{119}\text{Sn}$ at 50 MeV/u as described by the SMF model. In this way one can discuss the possible occurrence of statistical equilibrium even for a more explosive system, having a considerable amount of radial collective flow. Important differences between the two reactions are supposed to appear. Since at 50 MeV/u the emitted fragments are

generally smaller, one can find a large variety of source configurations that can fit the fragment partitions. However, we will show that the analysis of the corresponding fragment kinetic properties allows to clearly identify a unique solution.

II. BRIEF REVIEW OF THE EMPLOYED MODELS

Let us first give a brief description of the two models involved in this analysis. According to the SMF theory [6], during the expansion phase that follows the initial collisional shock the system encounters volume (spinodal) and/or surface instabilities, that lead to its break-up into many pieces. As in mean-field approaches, the system is represented by the one-body distribution function in phase space, that evolves according to the self-consistent nuclear (+ Coulomb) potential and to the stochastic collision integral, that accounts for the residual two-body interaction. In the approach considered, fluctuations are introduced in an approximate way [6]. Their amplitude is essentially determined by the degree of thermal agitation present in the system. Then fluctuations are amplified by the unstable mean-field, leading to the formation of fragments, whose properties reflect the structure of the most unstable collective modes. Several multipoles are excited with close probabilities, leading to a large variety of fragment configurations.[10].

Concerning more technical aspects, such as fragment recognition, we follow a coalescence procedure of the one-body density. Fragment excitation energies are calculated adopting the local density approximation, by subtracting the Fermi motion (associated with the local density) from the fragment kinetic energy (taken in the fragment reference frame) [10, 11].

The MMM model [5] describes the break-up of a statistically equilibrated nuclear source defined by the parameters: mass number (A), atomic number (Z), excitation energy (E) and freeze-out volume (V). The model as-

sumes equal probability between all configurations C : $\{A_i, Z_i, \epsilon_i, \mathbf{r}_i, \mathbf{p}_i, i = 1, \dots, N\}$ (the mass number, the atomic number, the excitation energy, the position and the momentum of each fragment i of the configuration C , composed of N fragments) subject to microcanonical constraints: $\sum_i A_i = A$, $\sum_i Z_i = Z$, $\sum_i \mathbf{p}_i = 0$, $\sum_i \mathbf{r}_i \times \mathbf{p}_i = 0$, E - constant. The level density of a given fragment (entering the statistical weight of a configuration) is taken to be of Fermi-gas type adjusted with the cut-off factor $\exp(-\epsilon/\tau)$: $\rho(\epsilon) = \rho_0(\epsilon) \exp(-\epsilon/\tau)$ [12] that counts for the dramatic decrease of the lifetime of fragment excited states respective to the freeze-out specific time as the excitation energy increases. MMM can work within two freeze-out hypotheses: (1) fragments are treated as hard spheres placed into a spherical freeze-out recipient and are not allowed to overlap each-other or the recipient wall; (2) fragments may be deformed and a corresponding free-volume expression is approaching the integration over fragment positions [12]. Hypothesis (2) is more adequate for the present study since it allows exploration of higher density configurations. Indeed, our dynamical studies seem to indicate that a good amount of statistical equilibrium is reached at a pre-fragment level, i.e. when the produced fragments are not fully separated yet [9]. This condition cannot be always matched by the space configurations related to the hypothesis (1), which presents severe constraints for low freeze-out volumes. Moreover, as resulting from [12], at relatively small freeze-out densities the results of the two approaches roughly coincide. This is why we perform the present investigation within hypothesis (2). The model employs a Metropolis-type simulation for estimating the average value of any system observable (see Refs. [5] for more details). While MMM includes a secondary decay stage, this stage is not necessary for the present analysis because we aim at a direct investigation of the (primary) *break-up* stage. A feature of this model, particularly important for the present study is the possibility of including *flow* in the primary decay stage. We include a standard flow velocity profile $v = v_0(r/R)^\alpha$ [12], where r is the distance of a given fragment from the system c.m. and R is the freeze-out recipient radius. In MMM the total flow energy is *microcanonically* conserved. Therefore, v_0 is evaluated for each fragmentation event from the condition of conservation of the system flow energy. The flow exponent α will be varied between the values 1 and 2.

III. STATISTICAL ANALYSIS

Using MMM we perform the analysis proposed in Ref. [9] in order to identify a possible statistical equilibration stage in the dynamical path of the reaction $^{129}\text{Xe} + ^{119}\text{Sn}$ at 50 MeV/u as provided by SMF. Within SMF the *dynamical freeze-out* time is defined as the time when the fragment formation process is over and therefore (intermediate mass) fragment multiplicities do not evolve any

longer. This time was identified to be around 200 fm/c.

In order to wash-up pre-equilibrium effects, which should appear in the dynamical simulation, only intermediate mass fragments (IMF) (i.e. fragments with $Z \geq 3$) are considered from both SMF and MMM simulations. Due to the large Coulomb repulsion among primary fragments and the possible presence of a collective flow, it is reasonable to assume that from the *equilibrated freeze-out*, i.e. the time when the system could have reached full phase space occupation, to the readily identified *dynamical freeze-out* the major difference will be the volume in which fragments are located. In other words we consider that all source variables except *volume* are roughly preserved. The fragment properties included in our analysis are connected to relevant inclusive observables that can be predicted by both models: fragment multiplicity and distributions and fragment internal excitation energy. We will fit these properties, but *not* the volume. For finding the best fit we have to minimize the following error function [9]:

$$\begin{aligned} \mathcal{E}_1 = & \{3[f(\langle A_{\text{bound}} \rangle) + f(\langle Z_{\text{bound}} \rangle)] \\ & + \left[\sum_{N_{\text{IMF}}} f(\langle dN/dN_{\text{IMF}} \rangle) / \sum_{N_{\text{IMF}}} 1 \right] \\ & + f(\langle \epsilon_{\text{IMF}} \rangle) + \sum_{i=1}^3 f(\langle Z_{\text{maxi}} \rangle) / 3\} / 9 \end{aligned} \quad (1)$$

where $\langle \cdot \rangle$ stands for average, A_{bound} and Z_{bound} are the bound mass and charge (sum of the mass number and, respectively, atomic number of all IMF's from a given event), N_{IMF} is the number of IMF's, ϵ_{IMF} is the fragment excitation energy per nucleon and Z_{maxi} with $i = 1, 2, 3$ are the largest, second largest and third largest charge from one fragmentation event. Further, $f(x) = |2(x_s - x_d)/(x_s + x_d)|$, where the indexes s and d stand for “statistic” and “dynamic”.

For finding the coordinates of the minimum of \mathcal{E}_1 we variate the MMM parameters A , E , V and τ in wide ranges thus constructing a four-dimensional grid. The ranges are $A : [170, 210]$, $E : [4, 8.5]$ MeV/u, $V/V_0 : [2, 14]$, $\tau = 20, 50, 100, \infty$ MeV. The source is considered to have the A/Z ratio of the $^{129}\text{Xe} + ^{119}\text{Sn}$ reaction. Like for the case of the 32 MeV/u incident energy for a given value of τ one gets a unique minimum for \mathcal{E}_1 . This is illustrated in Fig. 1 where cuts in \mathcal{E}_1 corresponding to A_{min} and E_{min} are represented for two values of τ : 50, ∞ MeV (where the index ‘min’ refers to the coordinates of the minimum value of \mathcal{E}_1). However, apart from the $^{129}\text{Xe} + ^{119}\text{Sn}$ at 32 MeV/u reaction, in the present case one cannot get an unambiguous source identification only by minimizing \mathcal{E}_1 . Indeed, it is possible to find a solution for any value of the considered τ and, as resulting from Fig. 2, the curve representing the minimum value of \mathcal{E}_1 versus τ is rather flat. In other words, primary fragment distributions and their internal excitation energies are not sufficient for proving the occurrence of equilibrium.

So, in order to better identify the *equilibrated source* we

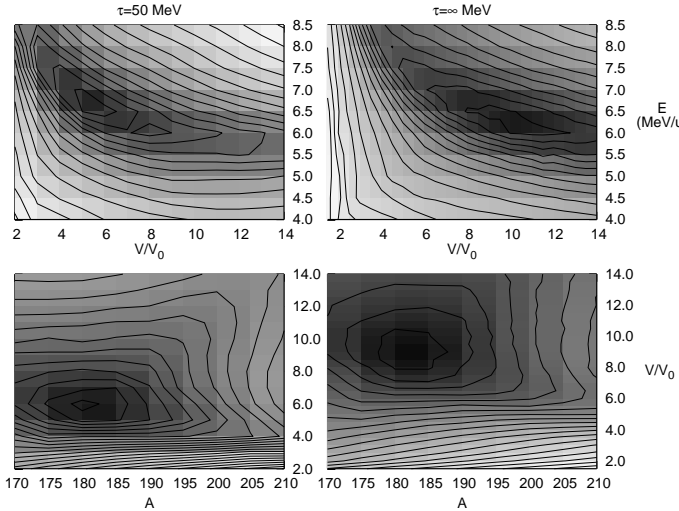


FIG. 1: Contour plots of the error function \mathcal{E}_1 [see eq. (1)] for $\tau = 50$ MeV (left column) and $\tau = \infty$ MeV (right column). Cuts in the $(V/V_0, E)$ (upper panel) and in the $(A, V/V_0)$ (lower panel) planes corresponding to the minimum \mathcal{E}_1 coordinates. Darker regions correspond to smaller \mathcal{E}_1 ; units are relative.

have to analyze the reaction kinematics too. More specifically, we fit the fragment kinetic distributions and the positions of the three highest charged fragments corresponding to the *dynamical freeze-out*. The error function employed in this fit is:

$$\mathcal{E}_2 = \left[\sum_{z=5}^{40} f(\langle k(z) \rangle) / 36 + \sum_{i=1}^3 f(\langle r(Z_{\max i}) \rangle) / 3 \right] / 2 \quad (2)$$

(k denotes the fragment kinetic energy and r denotes its position; in practice, for increasing the accuracy of the \mathcal{E}_2 estimator, a smoothed $k(z)$ curve was used and the z interval was spanned with a step of 5 units). But how can one get “statistical” information about the *dynamical freeze-out* in order to perform this fit? One simply has to propagate the primary fragments in their mutual Coulomb field, taking into account also the presence of collective flow effects, from their freeze-out positions as generated by MMM up to $\tilde{V}_{IMF} = 16.73 V_0$ which is the volume corresponding to the *dynamical freeze-out*. (Herein we use the notations from Ref. [9]: V is the volume of the smallest sphere which *totally* includes all fragments; \tilde{V} the volume of the smallest sphere which *totally* includes all fragments *and* has the center located in the center of mass of the system). Such propagations were performed for sources corresponding to the minimum \mathcal{E}_1 coordinates for each of the considered values of τ . The flow energy, $E_{fl} = \sum_i \frac{1}{2} m_i v_i^2$ (m_i and v_i being respectively the mass and the flow energy of the fragment i), and the flow exponent were varied in the ranges: $E_{fl} : [0, 1.6]$ MeV/u and $\alpha_{fl} : [1, 2]$. An unique minimum of the \mathcal{E}_2 function was found for each of the considered values of τ . One can observe this behavior in Fig. 3 for the case $\tau = \infty$. The obtained dependence of the \mathcal{E}_2

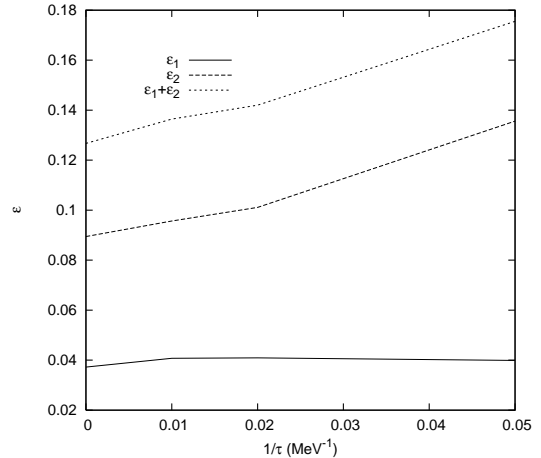


FIG. 2: The error functions \mathcal{E}_1 , \mathcal{E}_2 and $\mathcal{E} = \mathcal{E}_1 + \mathcal{E}_2$ versus $1/\tau$.

minima of τ is given in Fig. 2. This time we observe a monotonic dependence of $\mathcal{E}_{2\min}$ of τ . The global error function $\mathcal{E} = \mathcal{E}_1 + \mathcal{E}_2$ exhibits a well defined minimum as well (from now on we denote by \mathcal{E} this *minimum* value). This minimum corresponds to $\tau = \infty$.

It should be noticed that the full set of inclusive observables considered in the total estimator, \mathcal{E} , is quite exhaustive. Most of them coincide with the observables usually exploited in the comparison with experimental data.

For the sake of completeness, we test the \mathcal{E}_2 estimator in the case of the 32 MeV/u reaction, which was already analyzed in Ref. [9]. There it was shown that fragment kinetic energies and positions were compatible with the source identified only with \mathcal{E}_1 for a zero flow energy. In agreement with Ref. [9] results, the minimum of the \mathcal{E}_2 versus τ curve sharply points the value $\tau = \infty$, as \mathcal{E}_1 does, see Fig.4. In the (E_{fl}, α_{fl}) , $\tau = \infty$ plane \mathcal{E}_2 minimizes inside the $E_{fl}=0$ MeV region, as shown in Fig.5, which confirms the findings of Ref. [9]. The sharper minimum of the $\mathcal{E} = \mathcal{E}_1 + \mathcal{E}_2$ estimator observed for the 32 MeV/u reaction compared to the 50 MeV/u situation indicates a more advanced degree of statistical equilibrium reached in the 32 MeV/u reaction.

Finally, it is worth noticing that since hypothesis 1) of the MMM model induces artificial geometrical constraints at small volumes, it is easy to infer that, for example, in the case of 32 MeV/u one would not find any physically meaningful minimum (i.e. deep enough to insure a good reproduction of the data under study). On the other hand, for the 50 MeV/u reaction, the system being *less* affected by these constraints, the result would be closer to the evaluations obtained within hypothesis 2).

IV. INTERPRETING THE RESULTS

Some discussion is now in order for the 50 MeV/u reaction case: while mathematically speaking the absolute

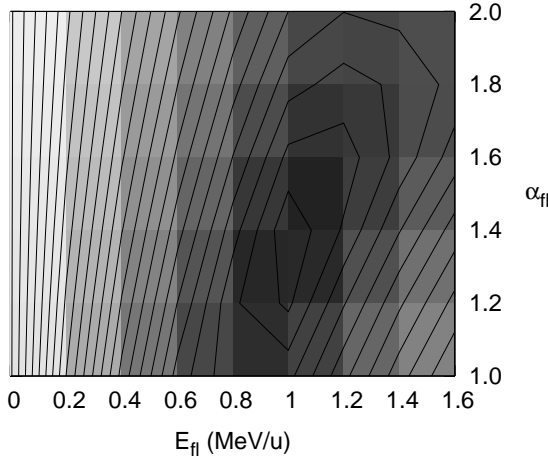


FIG. 3: Contour plot of the function \mathcal{E}_2 in the plane (E_{fl}, α_{fl}) corresponding to $\tau = \infty$. Units are relative; darker regions correspond to smaller values of \mathcal{E}_2 .

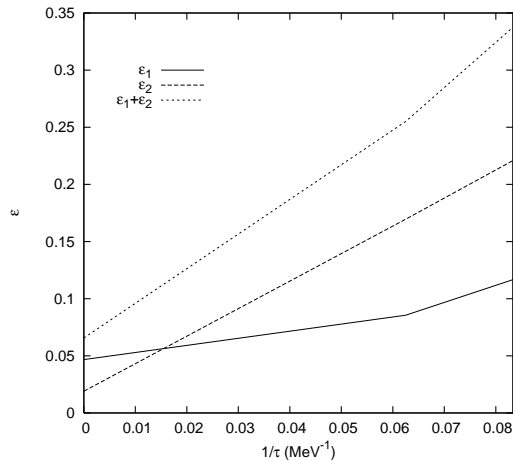


FIG. 4: The error functions \mathcal{E}_1 , \mathcal{E}_2 and $\mathcal{E} = \mathcal{E}_1 + \mathcal{E}_2$ versus $1/\tau$ for the case of the reaction Xe+Sn at 32 MeV/u.

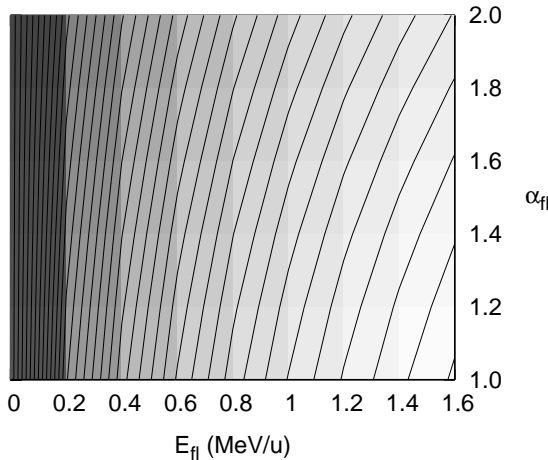


FIG. 5: Contour plot of the function \mathcal{E}_2 in the plane (E_{fl}, α_{fl}) for the case of the reaction Xe+Sn at 32 MeV/u. Units are relative; darker regions correspond to smaller values of \mathcal{E}_2 .

TABLE I: MMM: $\tau = 50$ MeV, ∞ versus SMF results for various system observables. $\langle \epsilon_{IMF} \rangle$ is given in MeV/u units.

Obs.	SMF	MMM: $\tau = 50$ MeV	MMM: $\tau = \infty$
$\langle A_{bound} \rangle$	159.2	159.3	156.4
$\langle Z_{bound} \rangle$	66.9	68.1	67.2
$\langle \epsilon_{IMF} \rangle$	3.65	3.64	3.65
$\langle Z_{max1} \rangle$	20.24	23.81	22.69
$\langle Z_{max2} \rangle$	13.85	14.92	15.03
$\langle Z_{max3} \rangle$	10.62	11.21	10.35

minimum corresponds indeed to $\tau = \infty$, one may observe a *plateau-like* behavior of this quantity starting at $\tau = 50$ MeV. It means that all values of τ between 50 MeV and ∞ are *almost equally* good solutions. An illustration of this fact is given in Fig. 6 where charge, number of intermediate mass fragments, kinetic energy and three highest charged fragment position distributions corresponding to $\tau = 50$ MeV and ∞ calculated with MMM are compared with the SMF results. The corresponding source parameters are: (1) $\tau = 50$ MeV, $A=183$, $Z=76$, $E=6.6$ MeV/u, $V/V_0=5.6$, $\tilde{V}/V_0=6.79$, $E_{fl}=0.6$ MeV/u, $\alpha_{fl}=1.2$, $t_p=58.8$ fm/c; (2) $\tau = \infty$, $A=183$, $Z=76$, $E=6.4$ MeV/u, $V/V_0=9.6$, $\tilde{V}/V_0=14.78$, $E_{fl}=1$ MeV/u, $\alpha_{fl}=1.4$, $t_p=14.8$ fm/c. (Here t_p denotes the propagation time, i.e. the time needed to reach, starting from the configuration predicted by MMM, the *dynamical freeze-out* configuration). The resemblance between the two cases transpires also from Table I, where the average value of some observables involved in the construction of \mathcal{E} , evaluated by MMM for $\tau = 50$ MeV, ∞ are compared with the corresponding SMF ones. In terms of time along the dynamical evolution, the $\tau = 50$ MeV and ∞ stages correspond respectively to approximately 140 fm/c and 185 fm/c. Note that for the 50 MeV/u reaction case, the agreement between dynamical and statistical radial distributions of the three largest fragments is weaker compared to the case of the 32 MeV/u reaction - see Fig. 7 (Ref. [9]).

But how to interpret these results? Which is the *real* equilibration time? Turning back to Fig. 2 we observe that the major change in \mathcal{E} versus τ occurred at $\tau = 50$ MeV. An interpretation would be that while a major part of the system phase space has already been spanned at $t = 140$ fm/c (i.e. $\tau = 50$ MeV), slight adjustments towards *equilibrium* are further achieved until $t = 185$ fm/c (i.e. $\tau = \infty$).

Two facts are strongly supporting this hypothesis: (1) As done for the 32 MeV case [9], one can perform, along the dynamical evolution, an analysis in terms of *pre-fragments*, i.e. try to identify density bumps (whose density is larger than the average) that will finally develop into the actual fragments observed at the *dynamical freeze-out* time [11, 13]. The SMF number of *pre-fragments* saturates at 140 fm/c (see Fig. 8). This is in agreement with Ref. [9] findings where the equilibration time for the $^{129}\text{Xe} + ^{119}\text{Sn}$ at 32 MeV/u was found to

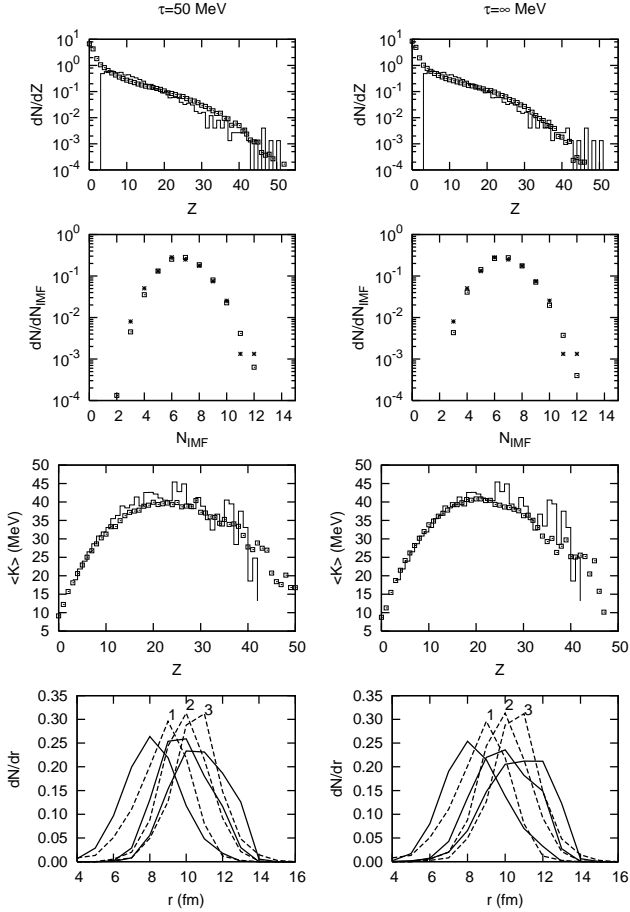


FIG. 6: From top to bottom: charge, number of intermediate mass fragments (IMF), kinetic, position of the first three highest charged fragment distributions (the position distributions are normalized by $4\pi r^2$). Left column: $\tau = 50$ MeV MeV; right column: $\tau = \infty$ MeV. MMM results (squares - first three rows from the top; solid line - last row) are plotted in comparison with the SMF ones. Results are corresponding to the $^{129}\text{Xe} + ^{119}\text{Sn}$ at 50 MeV/u reaction.

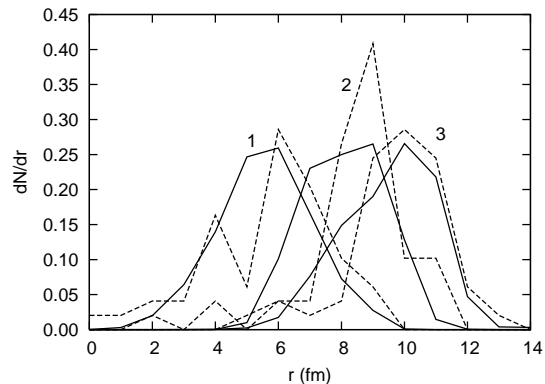


FIG. 7: Distributions of the position of the first three highest charged fragments (normalized by $4\pi r^2$). MMM results (solid line) are plotted in comparison with the SMF ones (dashed lines). Results correspond to the $^{129}\text{Xe} + ^{119}\text{Sn}$ at 32 MeV/u reaction [9].

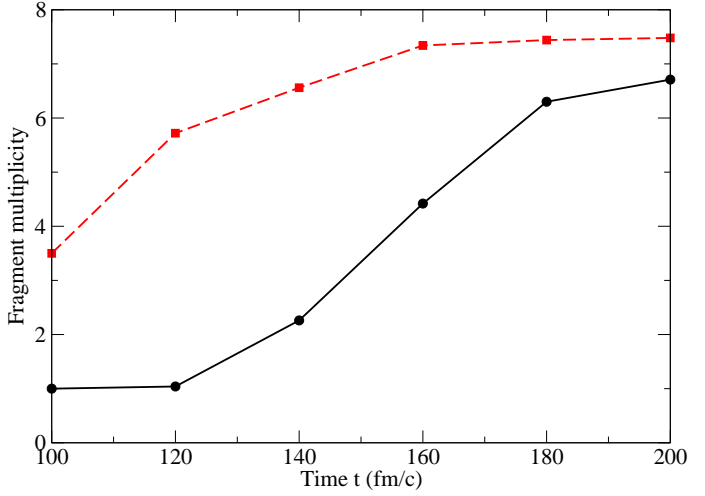


FIG. 8: (Color online) Dynamical results: Evolution of IMF (circles) and pre-fragment (squares+dashes) multiplicities in time.

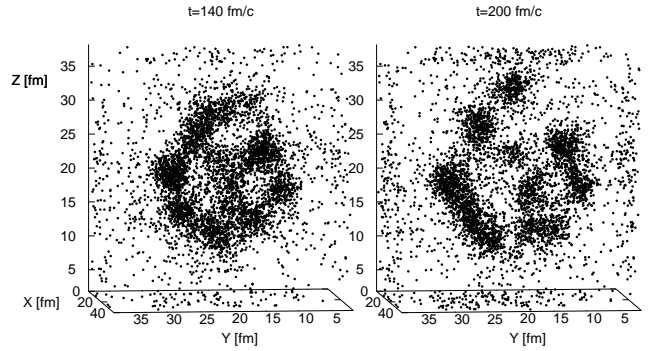


FIG. 9: Spatial distribution of test-particles in SMF corresponding to the moments of time 140 fm/c (left) and 200 fm/c (right) for an arbitrary fragmentation event.

coincide with the *pre-fragment* number saturation point.

(2) While at 140 fm/c the system is still in a pre-fragment stage, and therefore there is strong interaction between the fragment seeds, at 185 fm/c fragments are almost completely formed and separated. This is clearly illustrated by Fig.9 where fragment spatial configurations yielded by SMF, corresponding to the two moments of time are plotted. From this perspective, the further adjustments towards equilibrium taking place until 185 fm/c are achievable through a strongly decreasing nuclear inter-fragment interaction and Coulomb repulsion.

As a test for the validity of the analysis in terms of pre-fragments, we represent in Fig. 10 the distribution of the first three highest charged (*pre*)fragments for two moments of time: $t = 140$ fm/c and $t = 200$ fm/c. As it can be observed in Fig. 10 there is a perfect agreement between the distributions corresponding to the considered moments of time. This fact proves that the (*pre*)fragments partitions remain practically unchanged during the expansion from the *statistical freeze-out* to the *dynamical freeze-out*, nicely supporting the working hypothesis of our analysis.

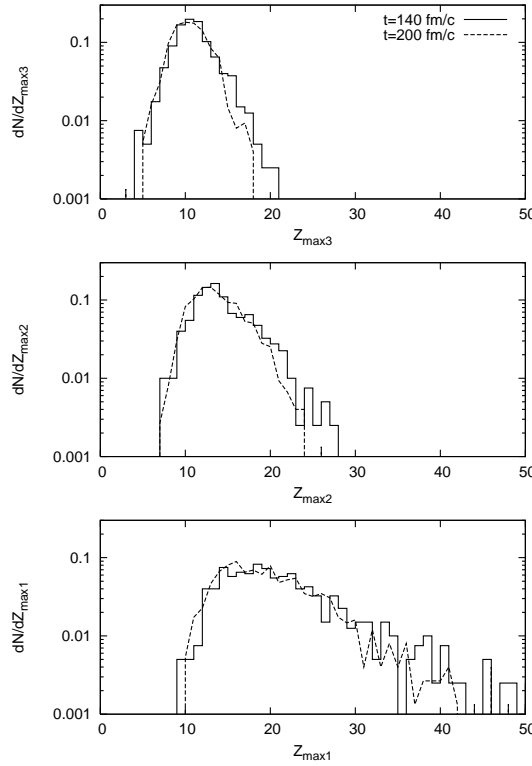


FIG. 10: Distributions of the first three highest charged *pre-fragments* corresponding to two moments of time of the reaction $\text{Xe}+\text{Sn}$ at 50 MeV/u. Full lines correspond to $t = 140 \text{ fm/c}$; dashed lines correspond to $t = 200 \text{ fm/c}$.

While fairly acceptable, the general agreement between the SMF results and the MMM ones for $^{129}\text{Xe}+^{119}\text{Sn}$ at 50 MeV/u reaction is weaker compared to the one corresponding to the $^{129}\text{Xe}+^{119}\text{Sn}$ at 32 MeV/u reaction. In the latter case the very good agreement between *statistical* and *dynamical* results for all the considered observables, is a strong indication of the system full equilibration. In particular, the distribution of the position of the three highest charged fragments, that is reported in Fig.7 for the 32 MeV/u case, is well reproduced, while the agreement is worse at 50 MeV/u (compare the bottom part of Fig.6 and Fig.7). Part of this difference is due to the approximations involved in both approaches. In fact, a 20% higher flow energy is observed at the *dynamical* freeze-out time as compared to the *statistical* one, suggesting some topological differences between the freeze-out partitions of the two approaches. The other part of it may be simply due to the fact that in the case of the 50 MeV/u reaction the system phase space is only *almost* spanned. This could be attributed to the fact that the present reaction is more violent compared to the 32 MeV/u one and, therefore, “more” dynamically driven. In this respect, see for example the more evident hollow configuration corresponding to the dynamical events (Fig.6-bottom panels and Fig.9).

V. FINAL REMARKS

Summarizing, the statistical analysis on the SMF dynamical path, started in Ref. [9], was extended to the $^{129}\text{Xe}+^{119}\text{Sn}$ at 50 MeV/u reaction. While most of the system configuration space appear to be already spanned at 140 fm/c, slight adjustments towards equilibration are further achieved until 185 fm/c.

The following conclusions about the statistical equilibration mechanism in dynamical paths can be drawn: 1) *equilibrium occurs while system constituents are still in interaction*; 2) *an external radial flow constraint is necessary at 50 MeV/u*. For both $^{129}\text{Xe}+^{119}\text{Sn}$ at 32 MeV/u [9] and 50 MeV/u reactions (most) of the equilibrium is already reached in a *pre-fragment* stage of the system. For both reactions this stage was found to coincide with the saturation of the *pre-fragment* number. Remarkably, this time is identical for both 32 MeV/u and 50 MeV/u reactions: phase space is spanned after the system has spent approximately 50 fm/c inside the unstable region of the liquid-gas phase diagram and corresponds to about 140 fm/c after the beginning of the reaction. Indeed, this time is related to the time scale of the instability growth towards the *pre-fragment* formation [6, 10]. However, the corresponding freeze-out volume is $5.6V_0$, much larger than the one corresponding to the 32 MeV/u reaction, due to the larger compression-expansion effects present in the 50 MeV/u reaction case. Further, it should be noticed that, while in the 32 MeV/u reaction case the equilibrated configuration corresponds to $\tau = \infty$ (see Ref. [9]), here, for the 50 MeV/u reaction, we find $\tau = 50 \text{ MeV}$. The physical meaning of this parameter, and its relation to the density and temperature conditions reached along the reaction path, need to be further investigated.

The present analysis reveals a qualitative difference between the 32 MeV/u and 50 MeV/u reactions: While in the 32 MeV/u case [9] fragment partitions and excitation energies impose strong constraints already identifying the equilibrated source, in the 50 MeV/u case, a subsequent kinematic analysis is necessary. This may be due to the higher amount of *liquid-like* phase in the 32 MeV/u reaction (see e.g. the more pronounced shoulder-like shape in the 32 MeV/u charge distribution of Ref.[9]), adding extra fragment-size related constraints to the 32 MeV/u events compared to the 50 MeV/u ones. This detail should be instructive for multifragmentation studies dealing with identifying the equilibrated sources by fitting the data with statistical models.

Finally, the present results may be useful for the experimental nuclear thermodynamics studies where volume is a key variable for locating the process in the phase diagram.

Acknowledgments

This work was supported by the European Community under a Marie Curie fellowship, contract n. MEIF - CT

[1] W. Bauer and A. Botvina, Phys. Rev. C **52**, R1760 (1995).

[2] D. H. E. Gross, Rep. Progr. Phys. **53**, 605 (1990).

[3] J. P. Bondorf, A. S. Botvina, A. S. Iljinov, I. N. Mishustin and K. Sneppen, Phys. Rep. **257**, 133 (1995).

[4] J. Randrup and S. Koonin, Nucl. Phys. **A471**, 355c (1987).

[5] Al. H. Raduta and Ad. R. Raduta, Phys. Rev. C **55**, 1344 (1997).; Al. H. Raduta and Ad. R. Raduta, Phys. Rev. C **61**, 034611 (2000).

[6] M. Colonna et al, Nucl. Phys. **A642**, 449 (1998).

[7] J.D. Frankland et al., Nucl. Phys. **A689**, 940 (2001); G. Tabacaru et al., Eur. Phys. J. **A18**, 103 (2003).

[8] M. Colonna, G. Fabbri, M. Di Toro, F. Matera, H. H. Wolter, Nucl. Phys. **A742**, 337 (2004).

[9] A. H. Raduta, M. Colonna, V. Baran and M. Di Toro, Phys. Rev. C **74**, 034604 (2006).

[10] Ph. Chomaz, M. Colonna, J. Randrup, Phys. Rep. **389**, 263 (2004).

[11] A. Guarnera et al., Phys. Lett. **B403**, 191 (1997).

[12] Al. H. Raduta and Ad. R. Raduta, Phys. Rev. C **65**, 054610 (2002).

[13] C.O. Dorso and J. Randrup, Phys. Lett. **B301**, 328 (1993).

[14] M. D'Agostino et al. Phys.Lett. B473 (2000) 219-225